

RESEARCH ARTICLE

A plasma diagnostic model of human T-cell leukemia virus-1 associated myelopathy

Makoto Ishihara¹, Natsumi Araya², Tomoo Sato², Naomi Saichi¹, Risa Fujii¹, Yoshihisa Yamano² & Koji Ueda¹¹Division of Biosciences, Functional Proteomics Center, Graduate School of Frontier Sciences, The University of Tokyo, Tokyo, Japan²Department of Rare Diseases Research, Institute of Medical Science, St. Marianna University School of Medicine, Kawasaki, Japan

Correspondence

Koji Ueda, Division of Biosciences, Functional Proteomics Center, Graduate School of Frontier Sciences, The University of Tokyo, CREST hall 1F, Institute of Medical Science, 4-6-1 Shirokanedai, Minato-ku, Tokyo, Japan, 108-8639. Tel: +81-3-6409-2062; Fax: +81-3-6409-2063; E-mail: k-ueda@ims.u-tokyo.ac.jp

Funding Information

This work was supported by grant-in-aid for Research Project on Overcoming Intractable Diseases from the Ministry of Health Labour and Welfare Japan and grant-in-aid for Young Scientists (B) (23701090) from the Ministry of Education, Culture, Sports, Science & Technology Japan.

Received: 19 November 2014; Accepted: 9 December 2014

Annals of Clinical and Translational Neurology 2015; 2(3): 231–240

doi: 10.1002/acn3.169

Abstract

Objective: Human T-cell leukemia virus-1 (HTLV-1) associated myelopathy/tropic spastic paraparesis (HAM/TSP) is induced by chronic inflammation in spinal cord due to HTLV-1 infection. Cerebrospinal fluid (CSF) neopterin or proviral load are clinically measured as disease grading biomarkers, however, they are not exactly specific to HAM/TSP. Therefore, we aimed to identify HAM/TSP-specific biomarker molecules and establish a novel less-invasive plasma diagnostic model for HAM/TSP. **Methods:** Proteome-wide quantitative profiling of CSFs from six asymptomatic HTLV-1 carriers (AC) and 51 HAM/TSP patients was performed. Fourteen severity grade biomarker proteins were further examined plasma enzyme-linked immunosorbent assay (ELISA) assays ($n = 71$). Finally, we constructed three-factor logistic regression model and evaluated the diagnostic power using 105 plasma samples. **Results:** Quantitative analysis for 1871 nonredundant CSF proteins identified from 57 individuals defined 14 CSF proteins showing significant correlation with Osame's motor disability score (OMDS). Subsequent ELISA experiments using 71 plasma specimens confirmed secreted protein acidic and rich in cysteine (SPARC) and vascular cell adhesion molecule-1 (VCAM-1) demonstrated the same correlations in plasma ($R = -0.373$ and $R = 0.431$, respectively). In this training set, we constructed a HAM/TSP diagnostic model using SPARC, VCAM1, and viral load. Sensitivity and specificity to diagnose HAM/TSP patients from AC (AC vs. OMDS 1–11) were 85.3% and 81.1%, respectively. Importantly, this model could be also useful for determination of therapeutic intervention point (OMDS 1–3 + AC vs. OMDS 4–11), exhibiting 80.0% sensitivity and 82.9% specificity. **Interpretation:** We propose a novel less-invasive diagnostic model for early detection and clinical stratification of HAM/TSP.

Introduction

The RNA retrovirus human T-cell leukemia virus-1 (HTLV-1) is endemic in Japan, Caribbean basin, Iran, Africa, South America, and the Melanesian islands.¹ Number of infected individuals is currently estimated at around 30 million worldwide,² in which 5% of virus carriers develop HTLV-1 associated myelopathy/tropic spastic paraparesis (HAM/TSP) or adult T-cell leukemia (ATL) after asymptomatic phase of typically over 30 years. Inflammation of spinal cord is a principal symptom of HAM/TSP patients, causing progressive sclerolytic,

gait impairment, or urination disorder.³ However, no curative therapy for HAM/TSP has been developed except for anti-inflammatory treatments by INF- α or steroids,⁴ whereas excessive or long-term use of these drugs can increase the risk of adverse events.^{5,6} Hence, the treatment regimens should be carefully managed based on a thorough assessment of disease stage and activity. As for the severity grading of HAM/TSP, Osame's motor disability score (OMDS) is widely used to define disease stages and estimate the rate of disease progression.⁷ Although this scale is helpful to evaluate consequential impairment of motor functions, development of molecular-based

diagnostics has been a major challenge for early detection and adequate therapeutic intervention of HAM/TSP.

To identify HAM/TSP-specific biomarkers, a variety of genomic or proteomic analyses were performed for infected T cells and plasma samples,^{8–10} however, comprehensive investigation for cerebrospinal fluid (CSF) has not been launched in spite of the most fundamental site of HAM/TSP lesion. Therefore, we intended to acquire the first proteome-wide view of CSFs reflecting HAM/TSP-associated alteration of spinal cord microenvironment. Following the statistical identification of severity grade biomarkers from CSFs, we attempted to construct a HAM/TSP diagnostic model using less-invasive plasma specimens.

Subjects and Methods

Participants

CSF specimens (from 51 HAM/TSP patients and six asymptomatic carriers [ACs]) and plasma specimens (from 50 HAM/TSP patients and 55 ACs) were collected in St. Marianna University School of Medicine and kept frozen at -80°C until just before use. The research procedure was explained and written informed consent was obtained from all the patients. This study was approved by the Ethical Committee of the University of Tokyo (approval code 14-1) and the Ethical Committee of St. Marianna University School of Medicine.

LC/MS/MS analysis

The 20 μL each of CSFs was lyophilized and dissolved in 8 mol/L Urea (GE Healthcare, Buckinghamshire, UK) in 50 mmol/L ammonium bicarbonate (Sigma-Aldrich, St. Louis, MO). After reduction with 5 mmol/L tris(2-carboxyethyl)phosphine (Sigma-Aldrich) at 37°C for 30 min, proteins were alkylated with 25 mmol/L Iodoacetamide (Sigma-Aldrich) at ambient temperature for 45 min. Following fourfold dilution with 50 mmol/L ammonium bicarbonate, proteins were digested with immobilized trypsin (Thermo Scientific, Bremen, Germany) at 37°C for 6 h. Digested samples were then desalted by Oasis HLB $\mu\text{Elution}$ plate (Waters, Milford, MA) and analyzed by liquid chromatography - tandem mass spectrometry (LC/MS/MS). The peptides were separated on Ultimate 3000 RSLC nano-HPLC system (Thermo Scientific) equipped with 0.075×150 mm C_{18} tip-column (Nikkyo Technos, Tokyo, Japan) using two-step linear gradient comprising 2–35% acetonitrile for 95 min and 35–95% acetonitrile for 15 min in 0.1% formic acid at the flow rate of 250 nL/min. The eluates were analyzed with LTQ Orbitrap Velos mass spectrometer (Thermo Scientific). Spectra were collected using full MS scan mode over the

mass-to-charge (m/z) range 400–1600. MS/MS was performed on the top 20 ions in each MS scan using the data-dependent acquisition mode with dynamic exclusion enabled.

2D-LC/MS/MS analysis

CSF tryptic digests were resolved in 10 mmol/L ammonium formate (Sigma-Aldrich) in 25% acetonitrile and fractionated with 0.2×250 mm strong cation exchange monolith column (GL Science, Tokyo, Japan). The samples were eluted with the gradient from 10 mmol/L to 1 mol/L of ammonium formate in curve = 3 mode within 70 min using Prominence HPLC system (Shimadzu Corporation, Kyoto, Japan). The eluate was separated into 11 fractions and analyzed by LC/MS/MS.

Protein/peptide identification

MS/MS spectra were searched against SwissProt database version 2012_06 (20,232 human protein sequences) using SEQUEST algorithm on ProteomeDiscoverer 1.3 software (Thermo Scientific). Proteins satisfying the false discovery rate (FDR) <1% by Peptide Validator FDR estimation algorithm on ProteomeDiscoverer was accepted. Gene ontology (GO) term analysis was performed using DAVID Bioinformatics Resources 6.7 (<http://david.abcc.ncifcrf.gov/>).

Label-free quantification analysis

The LC/MS/MS data from 57 CSF samples were imported on the Expressionist server (Genedata AG, Basel, Swiss) and processed along the workflow shown in Figure S1. The four-step Chromatogram Chemical Noise Subtraction was performed, composed of (1) RT structure removal = true, minimum RT length = 2 scans, (2) m/z structure removal = true, minimum m/z length = 6 scans, (3) RT window = 501 scans, quantile subtraction = 90%, and (4) RT structural removal = true, minimum RT length = 2 scans. Data points with intensity <500 were clipped to zero. Again, Chromatogram Chemical Noise Subtraction was performed using chromatogram smoothing = true, RT windows = 5 scans, and estimator = Moving average. After applying Chromatogram Grid with a distance of scan counts = 10, RT variety among 57 samples was normalized by Chromatogram RT Alignment: m/z windows = 11 points, RT windows = 11 scans, gap penalty = 1, RT search interval = 2 min, alignment scheme = pairwise alignment based tree. Peaks were detected by Chromatogram Summed Peak Detection: summation window = 20 scans, overlap = 10, minimum peak size = 6 scans, maximum merge distance = 1 point,

peak RT splitting = true, intensity profiling = maximum, gap/peak ratio = 5%, refinement threshold = 80, consistency threshold = 1. The detected peaks were grouped in isotopic clusters using Chromatogram Isotopic Peak Clustering: minimum charge = 1, maximum charge = 10, maximum missing peaks = 0, first allowed gap position = 10, RT window = 0.02 min, m/z tolerance = 5 ppm, isotope shape tolerance = 10, minimum cluster size ration = 0.5.

Cytometric bead array

Concentration of C-X-C motif chemokine 10 (CXCL10) in CSF was determined by cytometric bead array (CBA) (BD Biosciences, San Jose, CA) according to the manufacturer's instructions.

Enzyme-linked immunosorbent assay

Concentrations of secreted protein acidic and rich in cysteine (SPARC) (R&D Systems, Minneapolis, MN) and vascular cell adhesion molecule-1 (VCAM1) (Abcam, Cambridge, MA) in 105 plasma samples were measured with commercial enzyme-linked immunosorbent assay (ELISA) kit following the manufacturer's instructions. A multivariate logistic regression was applied to construct a new diagnostic model for HAM/TSP utilizing three factors, SPARC, VCAM1, and viral load, as described previously.¹¹

Result

Quantitative proteome profiling of CSFs from HAM/TSP patients

CSFs from 6 ACs and 51 HAM/TSP patients (Table 1) were processed according to the schematic workflow of this study (Fig. 1). Nonredundant 68,077 peptides from 57 individuals were detected and quantified on the Expressionist proteome server system, meanwhile 14,451

Table 1. Clinical characteristics of the CSF specimens.

Group	N	Age (\pm SD)	Gender (M/F)
AC	6	55.7 (\pm 15.8)	4/2
HAM1_3	7	57.9 (\pm 14.2)	3/4
HAM4_6	35	59.3 (\pm 11.0)	11/24
HAM7_11	9	61.6 (\pm 8.0)	1/8
Total	57	59.1 (\pm 11.7)	19/38

CSF, cerebrospinal fluid; AC, asymptomatic carriers; HAM1_3, HAM/TSP patients whose Osame's motor disability score from 1 to 3; HAM4_6, HAM/TSP patients whose Osame's motor disability score from 4 to 6; HAM7_11, HAM/TSP patients whose Osame's motor disability score from 7 to 11.

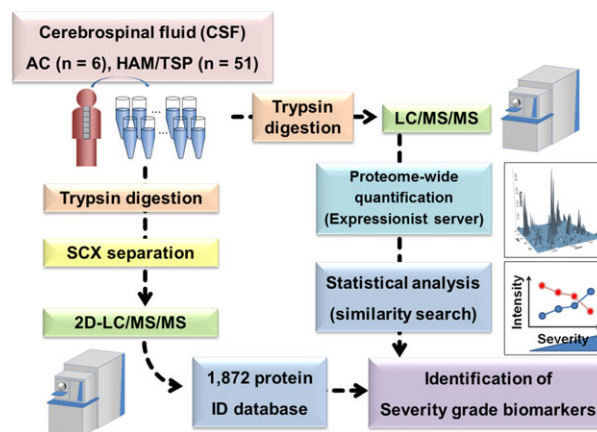


Figure 1. Schematic overview of severity grade marker screening. Cerebrospinal fluids (CSFs) from six asymptomatic carriers (ACs) and 51 HAM/TSP patients were analyzed by LC/MS/MS. Candidate peptides whose intensities had correlation with severity grades were isolated according to Pearson product-moment correlation coefficient. Candidate peptides were identified using Protein/Peptide identification database established by 2D-LC/MS/MS. HAM/TSP, human T-cell leukemia virus-1 associated myelopathy/tropic spastic paraparesis.

CSF peptides (1871 proteins) were identified by parallel 2D-LC/MS/MS analysis. To evaluate quantitative reliability of our LC/MS-based proteome profiling, observed relative concentrations of CXCL10 (Interferon gamma Inducible protein 10, CXCL10) were compared to clinical data which were measured by CBA (Fig. 2A). The result showed strong correlation ($R^2 = 0.911$) between two measurements, indicating that our LC/MS-based quantification results were highly credible even in the low concentration range (1–20 ng/mL).

Next, to interpret proteome-wide alterations in CSF environment of HAM/TSP patients, 1345 or 1750 proteins identified from AC or HAM/TSP patients group, respectively (Fig. 2B), were classified according to cellular component (CC, Fig. 2C and D) or biological process (BP, Fig. 2E and F) using DAVID Functional Annotation Tool. The CC analysis revealed that proteins expressed in cell projection and plasma membrane were enriched in CSF of HAM/TSP patients, in addition to specific enrichment of viral proteins. This may reflect increased invasive activity of HTLV-1-infected cells into spinal cord, which is often observed in HAM/TSP patients. Further BP analysis indicated that proteins involved in cell adhesion, cell motion, cell migration, cytoskeleton, and cell structure disassembly were highly enriched in CSF of HAM/TSP patients. These features also denoted proteome-wide environmental change in spinal cord, inducing active migration and/or invasion of lymphocytes. Proteins related to cell death and cell growth might associate with spinal inflammation in HAM/TSP patients.

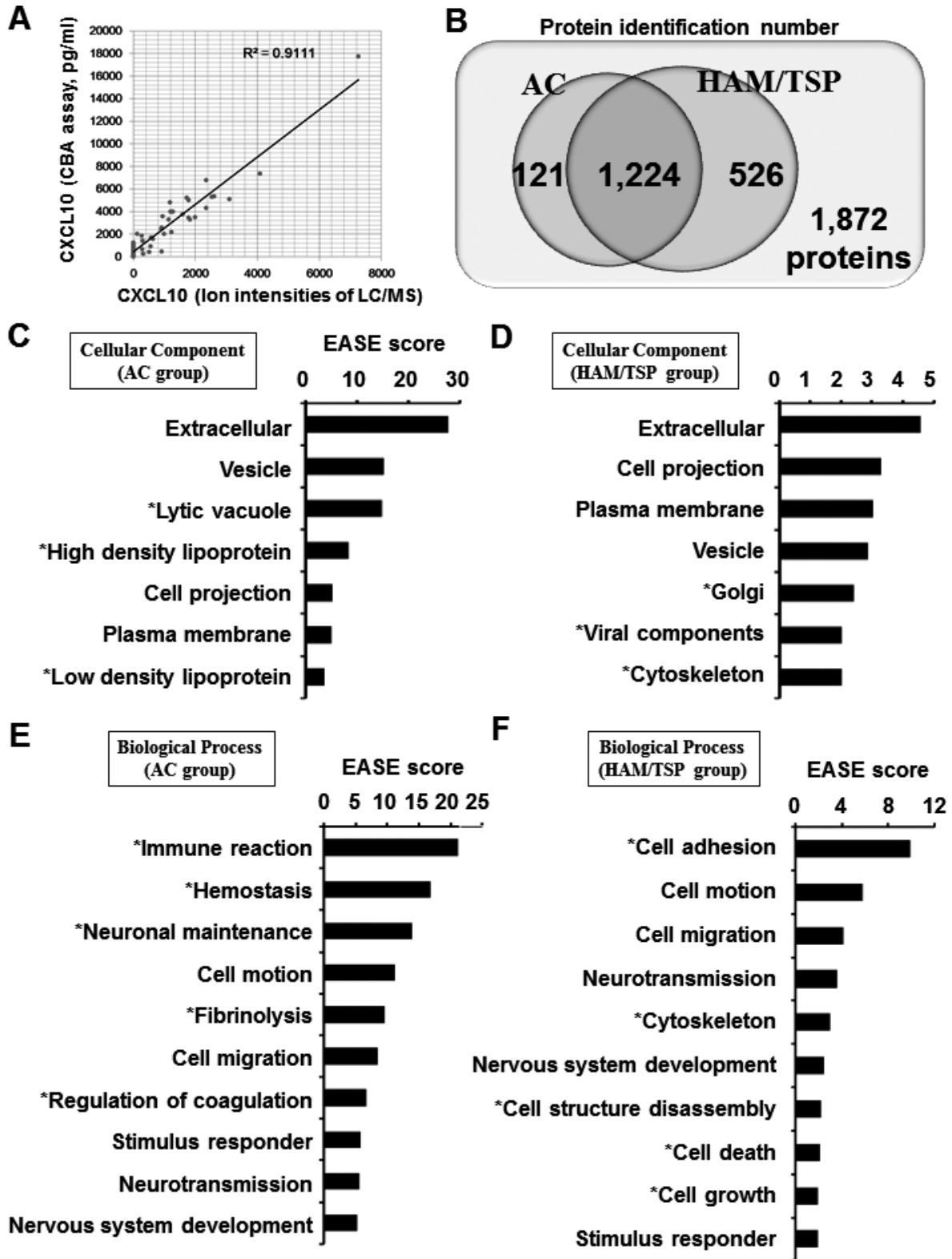


Table 2. List of 16 severity grade markers for HAM/TSP.

UniProt accession	Protein name	Amino acid numbers of identified peptide	Pearson's correlation coefficient (<i>R</i>)	<i>P</i> -value
Q9NZK5	Adenosine deaminase CECR1	247–258	0.478	5.15E-04
Q12860	Contactin-1	634–647	−0.425	9.94E-04
Q14118	Dystroglycan	222–232	−0.463	2.89E-04
Q8N2S1	Latent-transforming growth factor beta-binding protein 4	310–323	−0.463	2.90E-04
Q9Y5Y7	Lymphatic vessel endothelial hyaluronidic acid receptor 1	8–18	−0.499	9.15E-05
Q16653	Myelin-oligodendrocyte glycoprotein	14–25	−0.444	5.40E-04
Q9UJJ9	N-acetylglucosamine-1-phosphotransferase subunit gamma	47–56	−0.442	5.72E-04
P13591	Neural cell adhesion molecule 1	586–597	−0.459	3.31E-04
P36955	Pigment epithelium-derived factor	133–141	−0.454	3.83E-04
Q9UHG2	ProSAAS	14–24	−0.444	5.42E-04
P09486	Secreted protein acidic and rich in cysteine	124–133	−0.523	3.01E-05
P09486	Secreted protein acidic and rich in cysteine	156–164	−0.477	1.75E-04
P09486	Secreted protein acidic and rich in cysteine	252–262	−0.457	3.55E-04
Q92563	Testican-2	139–148	−0.424	1.03E-03
Q06418	Tyrosine-protein kinase receptor TYRO3	279–290	−0.438	1.04E-03
P19320	Vascular cell adhesion protein 1	581–590	0.430	9.35E-04

HAM/TSP, human T-cell leukemia virus-1 associated myelopathy/tropic spastic paraparesis.

Statistical analysis for screening severity grade marker candidates

To extract biomarker proteins showing stoichiometric increase/decrease in accordance with progression of HAM/TSP, numerical classes (0, 1, 2, and 3) were given to four clinically relevant severity groups (AC, HAM/TSP OMDS 1–3, 4–6, and 7–11, respectively) (see Table S1). Then quantitative correlation between severity classes and 68,077 peptide intensities was ranked with Pearson's correlation analysis. Peptides with the lowest 100 *P*-values (Table S2) were next subjected to protein identification analysis by 2D-LC/MS/MS, resulting in successful identification of 14 proteins derived from 16 peptides (Table 2). In addition to Pearson's correlation coefficients and *P*-values in Table 2, LC/MS-based quantitative profiles of 16 peptides were illustrated with box plots (Fig. 3). Compared to a traditional severity grade marker neopterin ($R = 0.4105$, $P = 1.12E-03$), any of identified proteins showed better potential to be utilized as CSF disease state biomarkers.

SPARC and VCAM-1 as HAM/TSP severity grade markers in plasma

To further narrow down the biomarker candidates and establish plasma-based less-invasive diagnostics, we examined plasma levels of the 14 proteins by ELISA assays measuring 71 training cases (Table 3). The results revealed that a couple of proteins, SPARC and VCAM1, showed the same correlation in plasma with CSF levels ($|R| > 0.4$ and $P < 0.05$) (Fig. 4A and B). Therefore, we attempted construction of the combination biomarker diagnostics using newly identified two proteins and HTLV-1 viral load, all of which are measurable from small volume of blood samples. In order to halt the progression of HAM/TSP and maintain better quality of life for patients, both early diagnosis of HAM/TSP onset and therapeutic intervention at appropriate time point are essential. On the basis of these clinical requirements, we made two logistic regression models which maximized area under the curve (AUC) of ROC curves comparing ACs with HAM/TSP patients (onset predictor; (1)) or

Figure 2. Summary of CSF proteome. (A) Evaluation of LC/MS-based quantification analysis. The relative concentrations of CXCL10 cytokine calculated by mass spectrometric analysis were compared to independent measurements by cytometric bead array (CBA). (B) Venn diagram of identified proteins in 57 CSF analyses. The Gene Ontology (GO) analysis using DAVID Bioinformatics Resources displayed enriched cellular components of CSF proteins in ACs (C) or HAM/TSP patients (D). The enriched biological functions of CSF proteins in ACs (E) or HAM/TSP patients (F) were also shown. Expression Analysis Systematic Explorer (EASE) enrichment scores were shown. CSF, cerebrospinal fluid; CXCL10, C-X-C motif chemokine 10; ACs, asymptomatic carriers; HAM/TSP, human T-cell leukemia virus-1 associated myelopathy/tropic spastic paraparesis.

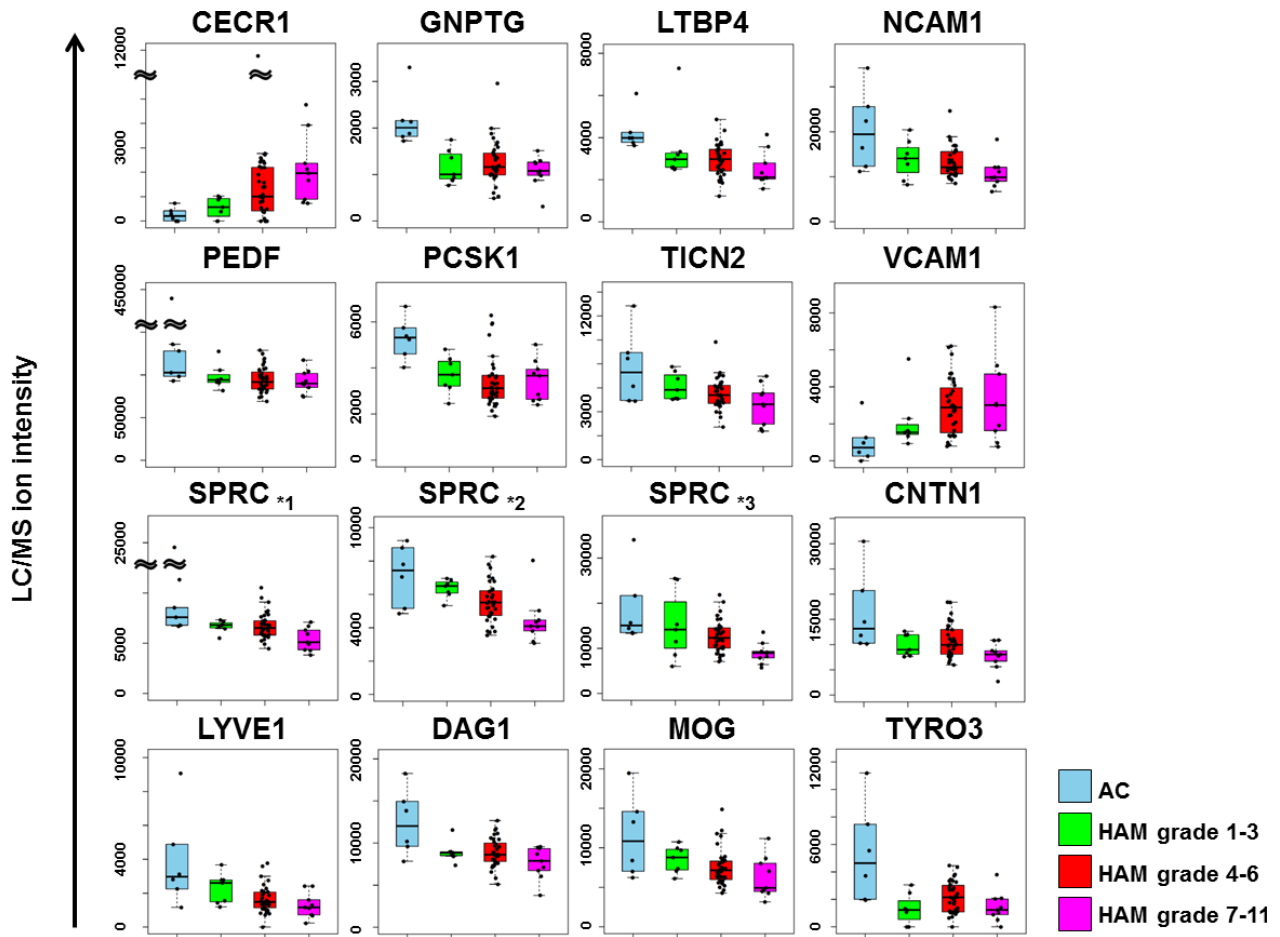


Figure 3. Panels of identified severity grade marker candidates for HAM/TSP. Box plots of 16 peptides derived from 14 candidate proteins are displayed. The Y axis stands for the LC/MS ion intensities. *1, *2, and *3 correspond to distinct SPARC-derived peptides. Amino acid numbers of peptides are as follows: *1; 124–133, *2; 156–164, *3; 252–262. HAM/TSP, human T-cell leukemia virus-1 associated myelopathy/tropic spastic paraparesis; SPARC, secreted protein acidic and rich in cysteine.

Table 3. Clinical characteristics of the plasma specimens.

Group	N	Age (±SD)	Gender (M/F)
Training cases			
AC	37	51.5 (±13.2)	13/24
HAM1_3	4	55.0 (±4.7)	3/1
HAM4_6	20	60.5 (±10.8)	4/16
HAM7_11	10	62.0 (±8.2)	2/8
Test cases			
AC	18	54.2 (±12.3)	4/14
HAM1_3	2	59.5 (±12.0)	0/2
HAM4_6	9	56.8 (±14.9)	4/5
HAM7_11	5	71.2 (±2.9)	0/5

AC, asymptomatic carriers; HAM1_3, HAM/TSP patients whose Osame’s motor disability score range from 1 to 3; HAM4_6, HAM/TSP patients whose Osame’s motor disability score range from 4 to 6; HAM7_11, HAM/TSP patients whose Osame’s motor disability score range from 7 to 11.

ACs + HAM/TSP OMDS 1–3 with HAM/TSP OMDS 4–11 (therapeutic intervention predictor; (2)).

$$\log\left(\frac{P(x)}{1-P(x)}\right) = -11.19 - 0.01980 (\text{SPARC}) + 0.009322 (\text{VCAM1}) + 0.1142 (\text{Viral Load}) \quad (1)$$

$$\log\left(\frac{P(x)}{1-P(x)}\right) = -11.73 - 0.01808 (\text{SPARC}) + 0.009651 (\text{VCAM1}) + 0.09151 (\text{Viral Load}) \quad (2)$$

Finally, we assessed our prediction models using 105 plasma samples (71 training samples with 34 independent test samples). The AUC of ROC curves in Figure 4C and D demonstrated significantly higher diagnostic powers of our three-factor models for both onset prediction

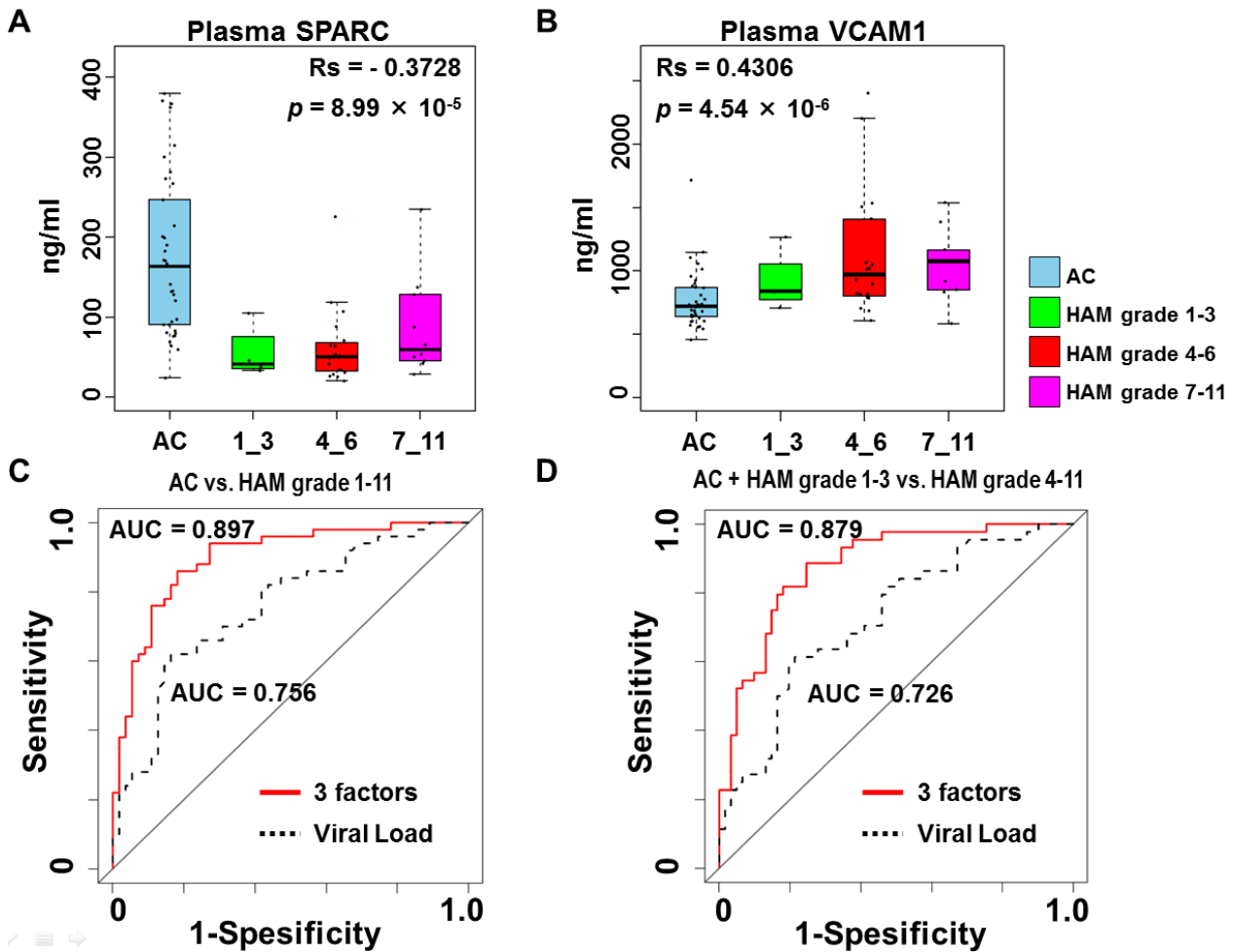


Figure 4. Construction of plasma-based diagnostic models. Plasma SPARC (A) and VCAM1 (B) were measured by ELISA assays. Pearson's correlation coefficient showed significant correlation between severity and novel markers. The three-factor logistic regression models (plasma SPARC, VCAM1, and HTLV-1 viral load) were validated with 105 samples in order for prediction of HAM/TSP onset (C) and appropriate therapeutic intervention point (D). The three-factor models showed better diagnostic performances than those of viral load only. Values of area under the curve (AUC) were shown. SPARC, secreted protein acidic and rich in cysteine; VCAM1, vascular cell adhesion molecule-1; ELISA, enzyme-linked immunosorbent assay; HTLV-1, human T-cell leukemia virus-1; HAM/TSP, human T-cell leukemia virus-1 associated myelopathy/tropic spastic paraparesis.

(AUC = 0.897) and treatment initiation point prediction (AUC = 0.879), compared to two-factor models (AUC = 0.861 and 0.856, respectively), SPARC (AUC = 0.748 and 0.736, respectively), VCAM1 (AUC = 0.768 and 0.774, respectively), and HTLV-1 viral load (AUC = 0.756 and 0.726, respectively) (Figs. S2, S3). Additionally, sensitivity and specificity of three-factor model for onset prediction were 86.0% and 81.8%, respectively, whereas those for treatment initiation point prediction were 81.8% and 82.0%, respectively (Table 4). These diagnostic yields were significantly better than those of previously reported biomarkers CSF neopterin, CSF CXCL10, and serum soluble IL-2 receptor (sIL-2R) (Table

S3). Thus, our three-factor diagnostics can provide valid and noninvasive routine test for HTLV-1 carriers and HAM/TSP patients, leading to precise disease control and better clinical outcome.

Discussion

An objective and scientifically evident diagnosis should be the basis of any medical actions. However, for HAM/TSP patients, clinical decisions have been made based on subjective health complaints mainly. Although HTLV-1 viral load, serum sIL-2R, and CSF neopterin are recently accepted as severity grade indicators for HAM/TSP,⁵ only

Table 4. Prediction of HAM/TSP onset and the point of therapeutic intervention.

Predictors	Onset					Point of therapeutic intervention				
	3 factors	SPARC + VCAM1	SPARC	VCAM1	Viral load	3 factors	SPARC + VCAM1	SPARC	VCAM1	Viral load
Training set (<i>n</i> = 71)										
Sensitivity %	85.3	82.4	76.5	79.4	55.9	80.0	73.3	76.7	60.0	53.3
Specificity %	81.1	67.6	45.9	62.2	89.2	82.9	80.5	48.8	85.4	82.9
Positive predictive value %	80.6	70.0	56.5	65.9	82.6	77.4	73.3	52.3	75.0	69.6
Negative predictive value %	85.7	80.6	68.0	76.7	68.8	85.0	80.5	74.1	74.5	70.8
AUC	0.897	0.839	0.669	0.754	0.732	0.881	0.846	0.667	0.773	0.699
Test set (<i>n</i> = 105)										
Sensitivity %	86.0	88.0	82.0	80.0	62.0	81.8	79.5	81.8	56.8	61.4
Specificity %	81.8	69.1	49.1	63.6	83.6	82.0	80.3	54.1	82.0	78.7
Positive predictive value %	81.1	72.1	59.4	66.7	77.5	76.6	74.5	56.3	69.4	67.5
Negative predictive value %	86.5	86.4	75.0	77.8	70.8	86.2	84.5	80.5	72.5	73.8
AUC	0.897	0.861	0.748	0.768	0.756	0.879	0.856	0.736	0.774	0.726

3 factors, logistic regression model using SPARC, VCAM1, and HTLV-1 viral load; HAM/TSP, human T-cell leukemia virus-1 associated myelopathy/tropic spastic paraparesis; AUC, area under the curve of ROC analysis.

relative increase/decrease of these biomarkers is valuable to assess efficiency of treatment. In this study, we successfully established predictive models which quantitatively define HAM/TSP disease status directly from plasma SPARC, VCAM1, and HTLV-1 viral load. This three-factor prediction model can be easily involved in routine medical examinations for ACs to monitor HAM/TSP onset because three biomarkers are measurable from a single blood collection without any invasive procedures such as CSF collection. Because progression of HAM/TSP tends to be rapid typically within a few years since the onset,¹² our prediction model for treatment initiation point will effectively prevent delay of deciding therapeutic intervention for early stage HAM/TSP patients.

Concerning physiological consideration of a new biomarker SPARC, the expression is specifically restricted within glial cells in nervous system including spinal cord.¹³ In addition, encephalitis induced by *N*-methyl-D-aspartic acid (NMDA) in mice resulted in downregulation of SPARC in glial cells.¹⁴ These facts suggested that plasma level of SPARC in HAM/TSP patients decrease along with the diminished number of glial cells caused by spinal cord degeneration and reduced expression of SPARC in glial cells which are pathological characteristics of HAM/TSP. On the other hand, CSF neopterin is known as an inflammatory small biological compound upregulated in many inflammatory neurologic diseases, such as multiple sclerosis, HIV encephalopathy, and Lyme neuroborreliosis,^{15–17} indicating that neopterin cannot describe spinal cord degeneration specifically. Therefore,

SPARC in plasma or CSF can be considered as more specific biomarker for HAM/TSP compared to CSF neopterin. Another new biomarker VCAM1 is expressed on the surface of endothelial cells, whose soluble form is known to be upregulated in plasma during the process of inflammation.¹⁸ In HAM/TSP patients, VCAM1 is upregulated in inflammatory region within spinal cord.¹⁹ Hence, diagnostic features of VCAM1 are more disease-oriented than neopterin, but VCAM1 can be measured from noninvasive blood specimens.

In conclusion, proteome-wide quantitative profiling of CSFs identified 14 severity grade biomarkers for HAM/TSP. Two of them, SPARC and VCAM1, were confirmed to be useful for plasma-based diagnosis of HAM/TSP onset and severity grades. It has long been difficult to expect a sudden onset of HAM/TSP after decades of asymptomatic phase in 0.5% of HTLV-1 carriers. Routine examination of our triple biomarkers will contribute to early diagnosis of HAM/TSP, leading to appropriate management of disease before suffering severe symptoms.

Acknowledgment

This work was supported by grant-in-aid for Research Project on Overcoming Intractable Diseases from the Ministry of Health Labour and Welfare Japan and grant-in-aid for Young Scientists (B) (23701090) from the Ministry of Education, Culture, Sports, Science & Technology Japan.

Conflict of Interest

Dr. Ueda has a patent Methods for detection and disease stage classification of HTLV-1 associated myelopathy pending. Dr. Ishihara has a patent Methods for detection and disease stage classification of HTLV-1 associated myelopathy pending. Dr. Araya has a patent Methods for detection and disease stage classification of HTLV-1 associated myelopathy pending. Dr. Saichi has a patent Methods for detection and disease stage classification of HTLV-1 associated myelopathy pending. Dr. Fujii has a patent Methods for detection and disease stage classification of HTLV-1 associated myelopathy pending. Dr. Sugano has a patent Methods for detection and disease stage classification of HTLV-1 associated myelopathy pending. Dr. Sato has a patent Methods for detection and disease stage classification of HTLV-1 associated myelopathy pending. Dr. Yamano has a patent Methods for detection and disease stage classification of HTLV-1 associated myelopathy pending.

References

1. Yamashita M, Ido E, Miura T, Hayami M. Molecular epidemiology of HTLV-I in the world. *J Acquir Immune Defic Syndr Hum Retrovirol* 1996;13(suppl 1):S124–S131.
2. Asquith B, Zhang Y, Mosley AJ, et al. In vivo T lymphocyte dynamics in humans and the impact of human T-lymphotropic virus 1 infection. *Proc Natl Acad Sci USA* 2007;104:8035–8040.
3. Enose-Akahata Y, Abrams A, Johnson KR, et al. Quantitative differences in HTLV-I antibody responses: classification and relative risk assessment for asymptomatic carriers and ATL and HAM/TSP patients from Jamaica. *Blood* 2012;119:2829–2836. doi: 10.1182/blood-2011-11-390807
4. Franzoi AC, Araujo AQ. Disability and determinants of gait performance in tropical spastic paraparesis/HTLV-I associated myelopathy (HAM/TSP). *Spinal Cord* 2007;45:64–68.
5. Yamano Y, Sato T. Clinical pathophysiology of human T-lymphotropic virus-type 1-associated myelopathy/tropical spastic paraparesis. *Front Microbiol* 2012;3:389. doi: 10.3389/fmicb.2012.00389
6. Kannagi M, Harashima N, Kurihara K, et al. Tumor immunity against adult T-cell leukemia. *Cancer Sci* 2005;96:249–255.
7. Shublaq M, Orsini M, Puccioni-Sohler M. Implications of HAM/TSP functional incapacity in the quality of life. *Arq Neuropsiquiatr* 2011;69(2A):208–211.
8. Semmes OJ, Cazares LH, Ward MD, et al. Discrete serum protein signatures discriminate between human retrovirus-associated hematologic and neurologic disease. *Leukemia* 2005;19:1229–1238.
9. Kirk PD, Witkover A, Courtney A, et al. Plasma proteome analysis in HTLV-1-associated myelopathy/tropical spastic paraparesis. *Retrovirology* 2011;8:81. doi: 10.1186/742-4690-8-81
10. Rahman S, Quann K, Pandya D, et al. HTLV-1 Tax mediated downregulation of miRNAs associated with chromatin remodeling factors in T cells with stably integrated viral promoter. *PLoS One* 2012;7:e34490. doi: 10.1371/journal.pone.0034490
11. Pepe MS, Cai T, Longton G. Combining predictors for classification using the area under the receiver operating characteristic curve. *Biometrics* 2006;62:221–229.
12. Taylor GP, Goon P, Furukawa Y, et al. Zidovudine plus lamivudine in human T-lymphotropic virus type-I-associated myelopathy: a randomised trial. *Retrovirology* 2006;3:63.
13. Vincent AJ, Lau PW, Roskams AJ. SPARC is expressed by macroglia and microglia in the developing and mature nervous system. *Dev Dyn* 2008;237:1449–1462.
14. Lloyd-Burton SM, York EM, Anwar MA, et al. SPARC regulates microgliosis and functional recovery following cortical ischemia. *J Neurosci* 2013;33:4468–4481.
15. Fredrikson S, Link H, Eneroth P. CSF neopterin as marker of disease activity in multiple sclerosis. *Acta Neurol Scand* 1987;75:352–355.
16. Karlsen NR, Froland SS, Reinvang I. HIV-related neuropsychological impairment and immunodeficiency. CD8+ lymphocytes and neopterin are related to HIV-encephalopathy. *Scand J Psychol* 1994;35:230–239.
17. Gasse T, Murr C, Meyersbach P, et al. Neopterin production and tryptophan degradation in acute Lyme neuroborreliosis versus late Lyme encephalopathy. *Eur J Clin Chem Clin Biochem* 1994;32:685–689.
18. Devaraj S, Glaser N, Griffen S, et al. Increased monocytic activity and biomarkers of inflammation in patients with type 1 diabetes. *Diabetes* 2006;55:774–779.
19. Izumo S. Neuropathology of HTLV-1-associated myelopathy (HAM/TSP). *Neuropathology* 2010;30:480–485.

Supporting Information

Additional Supporting Information may be found in the online version of this article:

- Table S1.** Osame's Motor Disability Score (OMDS).
Table S2. List of peptides with the lowest 100 *P*-values.
Table S3. Prediction of HAM/TSP onset and point of therapeutic intervention with existing markers.
Figure S1. Data acquired in LC/MS/MS analyses were loaded on Refiner MS and 2D-planes represented by mass-to-charge ratio and retention time were generated. To eliminate peaks originated from chemical noises on 2D-planes, four-step Noise Subtraction was conducted. All samples were aligned by retention times and 2D-planes

were merged into a single plane to determine peptide-derived peaks in Summed Peak Detection algorithm. Quantitative information accompanying each peptide was extracted after isotope clustering and statistical analyses were performed.

Figure S2. The classifiers for HAM/TSP onset established with two factors, SPARC and VCAM1 were appraised by

area under the curve of ROC curve. Red lines indicate the ROC curves of (A) two factors, (B) SPARC, and (C) VCAM1. Black broken lines show ROC curve of viral load.

Figure S3. The classifiers which distinguished HAM 4–11 from the others were evaluated by AUC. Red lines indicate ROC curves of (A) two factors, (B) SPARC, and (C) VCAM1. Black broken lines indicate viral load.